

Long-wavelength modes of cosmological scalar fields

Marcin Jankiewicz* and Thomas W. Kephart†

Department of Physics and Astronomy, Vanderbilt University, Nashville, Tennessee 37235, USA

(Received 22 March 2006; published 12 June 2006)

We give a numerical analysis of long-wavelength modes in the WKB approximation of cosmological scalar fields coupled to gravity via $\xi\phi^2R$. Massless fields are coupled conformally at $\xi = 1/6$. Conformality can be preserved for fields of nonzero mass by shifting ξ . We discuss implications for density perturbations.

DOI: [10.1103/PhysRevD.73.123514](https://doi.org/10.1103/PhysRevD.73.123514)

PACS numbers: 98.80.Cq

I. INTRODUCTION

Scalar fields have played a major role in attempts to model the early Universe. In particular, nearly every incarnation of the inflation scenario has relied on scalars to generate vacuum energy and in turn exponential expansion and density fluctuations. Many of these models rely on slow roll potentials, i.e., potentials that are nearly flat where the scalar masses can be very small.

Recently, horizon size and super horizon size density perturbations have been studied intensively, because of their importance for understanding low ℓ modes (see [1] and references therein) in the WMAP data [2]. Long-wavelength scalar-field modes have interesting properties when the wavelength is on the order of the horizon size cH_0^{-1} . One finds dispersion and diffraction effects that depend on the scalar mass and its coupling to gravity. The generic lagrangian for a scalar in a Friedmann-Robertson-Walker (FRW) Universe is

$$\mathcal{L} = g^{\mu\nu} \partial_\mu \phi \partial_\nu \phi + \xi \phi^2 R - V(\phi). \quad (1)$$

If $V(\phi)$ contains no dimensionful parameters, then the scalar field is conformally coupled when $\xi = \frac{1}{6}$. Conformal invariance can be broken by including a mass term in $V(\phi)$. Here we assume the local (Minkowski limit) real ϕ^4 theory is renormalizable. While this is not completely general, it is sufficient for our purposes. One could easily generalize our analysis to complex fields or fields in irreducible representations of some continuous symmetry group.

One expects the scalars to be an integral part of any realistic model, so for instance, if the overarching theory is based on strings with a global SUSY preserved down to some scale, then the scalars will be components of some superfield Φ contributing to the superpotential $W(\Phi)$. This will put constraints on $V(\phi)$. In particular, flat directions could result (regions of moduli space where the scalar mass vanishes) and lead to massless or nearly massless modes, where, for example, SUSY could be broken by nonperturbative effects. We give these comments as a justification

for the study of scalar zero modes and modes of very small positive mass or modes of very small imaginary mass (where the field could be rolling). However, there could be other reasons to study such modes.

As the wavelength approaches the horizon size, the naive redshift formula no longer applies and one must refine the flat space analysis of the scalar-field dispersion relation [3,4], see also [5–8]. We will carry out a numerical analysis of the behavior of long-wavelength scalar-field modes and investigate the dependence of the redshift on the scalar-field mass, and its coupling to gravity. We begin with a summary of scalar fields coupled to gravity in an FRW universe. We then review redshift and physical wavelength formulas, after which we are in position to begin our numerical analysis. We conclude with a discussion of the implications of our results.

The interpretation and application of our results requires some comments. The Universe has expanded through a number of phases during its lifetime. We think we are now transitioning from a matter-dominated phase to a vacuum-dominated phase. Earlier there was radiation domination, and before that, inflation, which occurred some time before big bang nucleosynthesis, but it is not clear how much before. Our task is to follow modes through these phases.

It is unlikely that long-wavelength modes can be measured directly so we are obliged to consider indirect measurements. These involve the long-wavelength background on which CMB or other short wavelength radiation propagates, and a proper analysis would consist of comparing observation with results predicted with and without dispersion.

Our best guess for the relevant long-wavelength modes that will lead to distortion of the CMB are those modes that were produced during inflation, then pushed outside the horizon during inflation, and have recently re-entered our horizon. These are the lowest ℓ modes. They will have their distortion preserved due of the fact that they have spent the time from which they left the horizon until the present epoch frozen, and so unable to grow or dissipate. Being of the order of the present horizon size, they will also display the maximum distortion. We give generic results that can be applied to any model, but since results are inflationary model dependent, a full analysis would require specifying model parameters ξ , m , etc.

*Electronic address: m.jankiewicz@vanderbilt.edu†Electronic address: thomas.w.kephart@vanderbilt.edu

II. SCALAR FIELDS COUPLED TO GRAVITY IN AN FRW UNIVERSE

We first review the properties of a real free massive scalar fields coupled to gravity. The most general action (to first order in R) for this case is [9]

$$S = \int d^4x \sqrt{-g} (g^{\mu\nu} \partial_\mu \phi \partial_\nu \phi - \xi \phi^2 R - m^2 \phi^2), \quad (2)$$

where R is the scalar curvature and ξ is a dimensionless coupling. We will work in FRW geometry, and use the convenient conformal parametrization of this family of spacetimes,

$$g_{\mu\nu} = C(\eta) \text{diag}(1, -h_{ij}(\mathbf{x})), \quad (3)$$

where $C(\eta) \equiv a^2(t)$ is the conformal scale factor related to a conformal time via

$$\eta(t) = \int^t \frac{cdt'}{a(t')}. \quad (4)$$

The spacial part of the metric is

$$h_{ij}(\mathbf{x}) = \text{diag}((1 - \kappa r^2)^{-1}, r^2, r^2 \sin^2 \theta), \quad (5)$$

with $\kappa = 0, 1, -1$ corresponding to (flat), deSitter (positive) or anti-de Sitter (negative) curved spatial sections, respectively.

The action (2) leads to the field equation

$$\square \phi + m^2 \phi + \xi \phi R = 0, \quad (6)$$

where $\square = \frac{1}{\sqrt{-g}} \partial_\mu (\sqrt{-g} g^{\mu\nu} \partial_\nu)$. Because of the homogeneity and isotropy of the FRW metric, the solution to the field equation factorizes to

$$\phi_k(\eta, \mathbf{x}) = C^{-1/2}(\eta) f_k(\eta) \mathcal{Y}_k(\mathbf{x}), \quad (7)$$

where \mathcal{Y}_k is an eigenfunction of the spatial Laplacian

$$\frac{1}{\sqrt{-h}} \partial_i [\sqrt{-h} h^{ij} \partial_j \mathcal{Y}_k(\mathbf{x})] = -(|\mathbf{k}|^2 - \kappa) \mathcal{Y}_k(\mathbf{x}), \quad (8)$$

and $k = |\mathbf{k}|$. In the massive case, the temporal part of (7) has to satisfy

$$\ddot{f}_k + \left[k^2 + m^2 C(\eta) + \xi - \frac{1}{6} R(\eta) C(\eta) \right] f_k = 0, \quad (9)$$

where the dot represents derivative with respect to conformal time η . One can express the scalar curvature R in terms of scale factor C and curvature constant κ in the form

$$\frac{1}{3} RC = \frac{\ddot{C}}{C} - \frac{1}{2} \left(\frac{\dot{C}}{C} \right)^2 + 2\kappa. \quad (10)$$

Thanks to this relation, Eq. (9) takes the form

$$\ddot{f}_k + \left\{ k^2 + m^2 C + 6 \left(\xi - \frac{1}{6} \right) \kappa + 3 \left(\xi - \frac{1}{6} \right) \left[\frac{\ddot{C}}{C} - \frac{1}{2} \left(\frac{\dot{C}}{C} \right)^2 \right] \right\} f_k = 0. \quad (11)$$

The theory is conformally coupled if $\xi = \frac{1}{6}$ and $m^2 = 0$. We will concentrate on two realistic cosmological regimes: vacuum (VDU) and matter (MDU) dominated epochs. In these cases (11) reduces to

$$\ddot{f}_k + \left[\beta^2 + m^2 C - \frac{\nu^2 - \frac{1}{4}}{\eta^2} \right] f_k = 0, \quad (12)$$

where we have introduced the index ν defined by

$$\nu^2(\xi, p) = \frac{1}{4} - (6\xi - 1) \frac{p(2p - 1)}{(p - 1)^2}, \quad (13)$$

with $p = 2/3$ for MDU and is also formally $2/3$ for VDU. We have also introduced a conformal wave number β , corresponding to a mode k :

$$\beta^2 = \left[\frac{4\pi^2}{\lambda_0^2} + (6\xi - 1)(\Omega_0 - 1)H_0^2 \right] a^2(t_0). \quad (14)$$

Here λ_0 denotes the physical wavelength, corresponding to the wave number k , as measured today, Ω_0 is the present ratio of matter-energy density to critical density and H_0 is the present value of the Hubble parameter. Since all current observational evidence points toward a flat universe, we set $\kappa = 0$ ($\Omega_0 = 1$) so that (14) reduces to

$$\beta = k = \frac{2\pi}{\lambda_0} a(t_0). \quad (15)$$

A. Massless case

In the massless case (12) reduces to Bessel's equation

$$\ddot{f}_k + \left[\beta^2 - \frac{\nu^2 - \frac{1}{4}}{\eta^2} \right] f_k = 0. \quad (16)$$

The solutions to this equation can be written in terms of Hankel functions $H_\nu^{(1)}(\beta\eta)$, which in polar form are

$$H_\nu^{(1)}(\beta\eta) = A(\beta\eta) e^{-iS(\beta\eta, \nu)}, \quad (17)$$

with A and S being real valued amplitude and phase functions. These are easily expressed in terms of ordinary Bessel functions J_ν and Bessel functions of the second kind Y_ν . The phase is

$$S(\beta\eta, \nu) = \arctan \frac{\cot(\pi\nu) J_\nu(\beta\eta) - \csc(\pi\nu) J_{-\nu}(\beta\eta)}{J_\nu(\beta\eta)}, \quad (18)$$

for real $\nu(\xi, p)$, i.e., for $\xi < 3/16$ in a case of $p = 2/3$ and

$$S(\beta\eta, \nu) = \arctan \frac{\Im[e^{-i\nu\pi} J_\nu(\beta\eta) - J_{-\nu}(\beta\eta)]}{\Re[e^{-i\nu\pi} J_\nu(\beta\eta) - J_{-\nu}(\beta\eta)]}, \quad (19)$$

for imaginary $\nu(\xi, p)$, i.e., for $\xi > 3/16$ for both MDU and VDU. The amplitude is

TABLE I. Important factors for VDU and MDU.

| | $a(t)$ | | | $\eta[a(t)]$ | $\eta(z)$ |
|-----|----------------------------|---|---|------------------------------------|--------------------------------------|
| VDU | $e^{a_{\text{vac}}^0 t}$ | $a_{\text{vac}}^0 = \left[\frac{8\pi G_N}{3} \rho_0(w) \Big _{w=-1} \right]^{1/2}$ | $a_{\text{vac}}^0 \simeq 2.27 \times 10^{-18} \text{ s}^{-1}$ | $\frac{c}{a_{\text{vac}}^0 a(t)}$ | $c a_{\text{vac}}^{0-1} (z+1)$ |
| MDU | $a_{\text{mat}}^0 t^{2/3}$ | $a_{\text{mat}}^0 = \left[6\pi G_N \rho_0(w) \Big _{w=0} \right]^{1/3}$ | $a_{\text{mat}}^0 \simeq 2.05 \times 10^{-18} \text{ s}^{-1}$ | $\frac{3c}{a_{\text{mat}}^0} a(t)$ | $2c a_{\text{mat}}^0 (1+z)^{-(1/2)}$ |

TABLE II. Zeroth order result for frequency, scale factor and their derivatives, where a given epoch is characterized by: w , the proportionality constant in the equation of state $P(t) = w\rho(t)$ appropriate for a given background, as well as the exponent of a power-law type cosmologies, i.e. $a(t) \sim t^p$.

| Epoch: (w, p) | $\omega_k^{(0)}$ | $\dot{\omega}_k^{(0)}$ | $a(t)$ | $C(\eta)$ | $\dot{C}(\eta)$ | $\ddot{C}(\eta)$ |
|-----------------------------|--|---|---|---|---|--|
| Vacuum: $(-1, \frac{2}{3})$ | $\sqrt{\beta^2 + m^2 \left(\frac{c}{a_{\text{vac}}^0}\right) \eta^{-2}}$ | $-\frac{m^2 \eta^{-3}}{\omega_k^{(0)}}$ | $\exp\left\{\left[\frac{8\pi G_N}{3} \rho_0\right]^{1/2} t\right\}$ | $\left(\frac{c}{a_{\text{vac}}^0}\right)^2 \eta^{-2}$ | $-2\left(\frac{c}{a_{\text{vac}}^0}\right)^2 \eta^{-3}$ | $6\left(\frac{c}{a_{\text{vac}}^0}\right)^2 \eta^{-4}$ |
| Matter: $(0, \frac{2}{3})$ | $\sqrt{\beta^2 + m^2 \frac{a_{\text{mat}}^0}{81c^4} \eta^4 \eta^4}$ | $2\frac{m^2 \eta^3}{\omega_k^{(0)}}$ | $[6\pi G_N \rho_0]^{1/3} t^{2/3}$ | $\frac{a_{\text{mat}}^0}{81c^4} \eta^4$ | $4\frac{a_{\text{mat}}^0}{81c^4} \eta^3$ | $12\frac{a_{\text{mat}}^0}{81c^4} \eta^2$ |

$$A(\beta\eta, \nu) = \sqrt{J_\nu^2(\beta\eta) + Y_\nu^2(\beta\eta)}, \quad (20)$$

for real ν , and for imaginary ν we find

$$A(\beta\eta, \nu) = |\csc(\pi\eta)| \sqrt{\{\Re[e^{-i\pi\nu} J_\nu(\beta\eta) - J_{-\nu}(\beta\eta)]\}^2 + \{\Im[e^{-i\pi\nu} J_\nu(\beta\eta) - J_{-\nu}(\beta\eta)]\}^2}. \quad (21)$$

The instantaneous angular frequency of FRW modes associated with a wave number k is given by

$$\omega_k = \frac{\partial S}{\partial \eta}, \quad (22)$$

where S is the corresponding phase given by either (18) or (19), depending on a value of coupling ξ and choice of cosmology.

B. Massive case

We want to write (11) in the form $\ddot{f}_k + \omega_k^2 f_k = 0$. Therefore using a WKB analysis one finds the frequency (22) to second order $\ddot{f}_k + \omega_k^{(2)2} f_k = 0$, where $\omega_k^{(2)}$ is given [4] by

$$\omega_k^{(2)}(\eta) = \omega_k^{(0)} + \frac{3\xi - \frac{1}{2}}{2\omega_k^{(0)}} \left[\frac{\ddot{C}}{C} - \frac{1}{2} \left(\frac{\dot{C}}{C} \right)^2 \right] - \frac{m^2}{8(\omega_k^{(0)})^3} \left[\ddot{C} - \dot{C} \frac{\dot{\omega}_k^{(0)}}{\omega_k^{(0)}} - \frac{3m^2}{4} \frac{\dot{C}^2}{(\omega_k^{(0)})^2} \right], \quad (23)$$

with

$$\omega_k^{(0)} = \sqrt{\beta^2 + m^2 C(\eta)}. \quad (24)$$

We have checked the validity of the WKB approximation (see Appendix A) by comparing with the massless limit where exact solutions are available. The zeroth order contributions to the frequency and conformal scale factor and their derivatives for the cosmological cases of interest are summarized in Table I.¹

¹In the following we take the value of the present energy density to be $\rho_0 = \rho_{\text{crit}} = 9.21 \times 10^{-27} \frac{\text{kg}}{\text{m}^3} \Rightarrow H_0^{-1} = a_{\text{vac}}^{0-1} = 4.42 \times 10^{17} \text{ s}$.

The scale factor and hence conformal time depends on the given epoch, so for power-law expansions we have

$$a(t) = [6\pi G_N (1+w)^2 \rho_0(w) t^2]^{1/(3(1+w))} \quad (25)$$

as can be directly determined from the Friedmann equation, where w is the proportionality constant in the equation of state $P(t) = w\rho(t)$ appropriate for a given background, and $\rho_0(w)$ is a present value of critical density for a given epoch. Relevant choices of parameters for use in (23) and (25) are given in Tables I and II.

C. Redshift formula

The classical redshift formula in terms of frequency ν is

$$\frac{\nu_0}{\nu} = \frac{a(t)}{a(t_0)}. \quad (26)$$

We want to find the correction factor to this naive redshift formula where the correction is the result of the nontrivial modifications to the dispersion relations for long-wavelength modes i.e., wavelengths of the order of the horizon size. To do this we have to take account of the conformal angular frequency correction [3] so that we find

TABLE III. Dictionary of conformal and physical variables.

| | Conformal | Physical |
|-------------|---|---|
| space | x | $x_{\text{phy}} = a(t)x$ |
| time | $\eta = \int^t \frac{cdt'}{a(t')}$ | t |
| wave vector | k | $k_{\text{phy}} = \frac{k}{a(t)}$ |
| wavelength | $\lambda = \frac{2\pi}{ k }$ | $\lambda_{\text{phy}} = a(t)\lambda$ |
| frequency | $\omega = \frac{\partial S}{\partial \eta}$ | $\omega_{\text{phy}} = \frac{\omega}{a(t)}$ |

$$\frac{\nu_0}{\nu} = \frac{a(t)}{a(t_0)} \frac{\omega_k(t_0)}{\omega_k(t)}. \quad (27)$$

$$z = \frac{a(t_0)}{a(t)} - 1, \quad (28)$$

and the parameter b_0

$$b_0 \equiv \frac{\lambda_0}{cH_0^{-1}}, \quad (29)$$

Here for ω_k we use $\omega_k^{(0)} = \beta$ in the massless case and $\omega_k^{(2)}$, given by Eq. (23), in the massive case. In the following sections we are going to present the results for two different cosmologies. The relations between physical and conformal variables are summarized in Tables I and III. The advantage of an analysis via the WKB method is that it is simple and straightforward, and it usually gives the correct trends when the corrections are moderate ($\sim 5\%$ to $\sim 20\%$) (as we have shown in Appendix A). These observations can be verified by comparing with exact results where they exist. In the cosmological regimes of relevance (vacuum and matter domination), we find the dependence of the dispersion relations on the value of the mass of the scalar field. We formulate our discussion in terms of conformal invariance, i.e., in terms of the value of the mass and wavelength where the conformal behavior is approximately preserved.

In all cases we find $m \sim 10^{-33}$ eV (inverse Hubble size) as the mass where nonconformal behavior starts to set in. These masses should be nearly equal in the different regimes, since differences are caused by numerical factors of order one.

To proceed further, we first have to express all the parameters present in Eqs. (23) and (24) in terms of redshifts

that can be interpreted as the fractional size of the physical wavelength in the units of the present Hubble radius. We will work in units where $a(t)$ and hence $C(\eta)$ are dimensionless. The wave number β does not depend on the epoch, as can be seen from Eq. (15). We have now collected all the necessary epoch specific input needed for our numerical analysis that will be carried out in the next section.

III. CORRECTION TO REDSHIFTS

In this section we are going to present corrections due to the redshift formula (27) originating from the coupling of the scalar fields to gravity. We consider massless as well as massive cases in two different cosmologies, i.e., vacuum and matter-dominated universes. In order to see the full spectrum of possible behavior of the dispersion relations, one has to discuss both real and imaginary masses. We plot the ratio of initial to final frequencies in each epoch. Sequentially through matter and vacuum domination, we set $z_i^{\text{mat}} = 1100$, next $z_f^{\text{mat}} = z_i^{\text{vac}} = 0.4$ (using correct WMAP value of $\Omega_\Lambda = 0.73$ [10]) and finally $z_f^{\text{vac}} = 0$. In the case of vacuum domination, for real masses Fig. 1, the

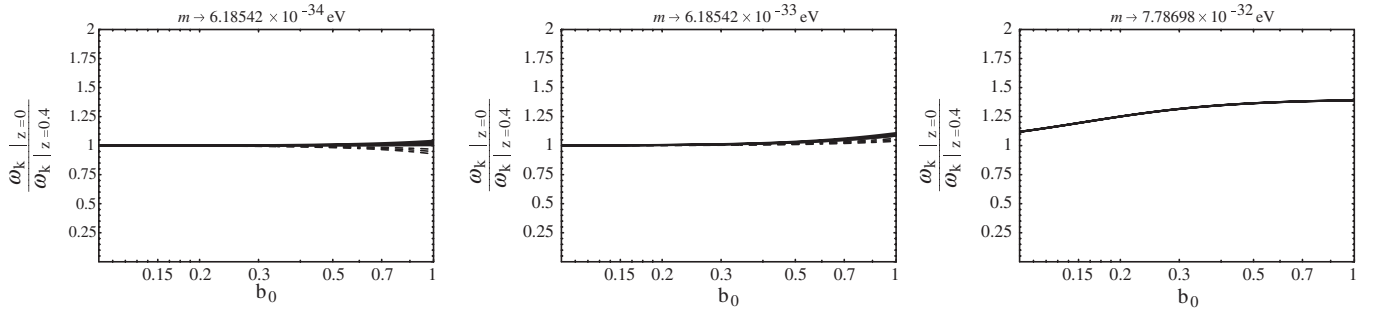


FIG. 1. Vacuum Domination $m^2 > 0$ WKB: Dashed curves $\xi < 1/6$, Thick curves $\xi > 1/6$. In this and the following figures we use $\xi = \pm 3/4, \pm 1/2, \pm 1/4, 0$ for ξ s.

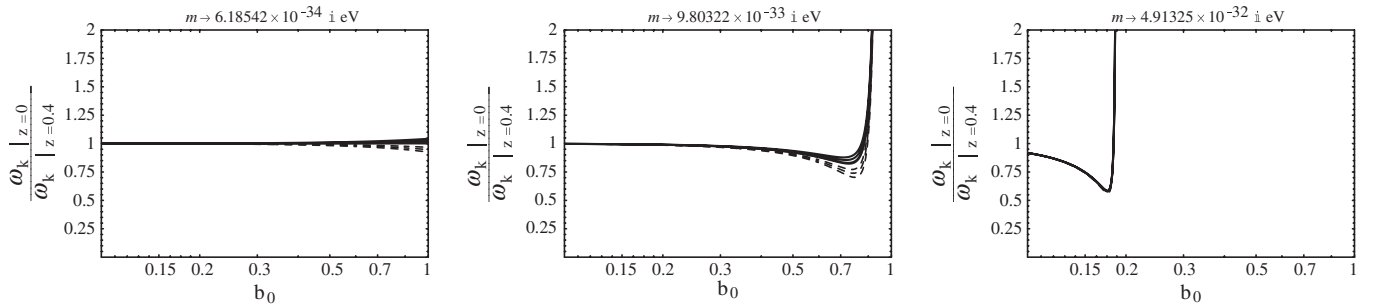


FIG. 2. Vacuum Domination $m^2 < 0$ WKB: Dashed curves are for $\xi < 1/6$, and thick curves are for $\xi > 1/6$.

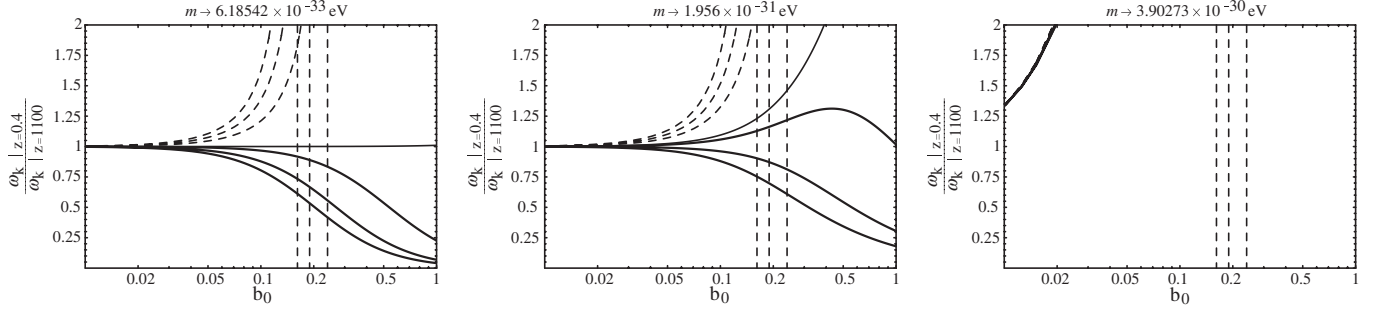


FIG. 3. Matter Domination $m^2 > 0$ WKB: Dashed curves are for $\xi < 1/6$, and thick curves are for $\xi > 1/6$. On this and the following figures vertical lines show the corresponding asymptotes where the WKB approximation fails.

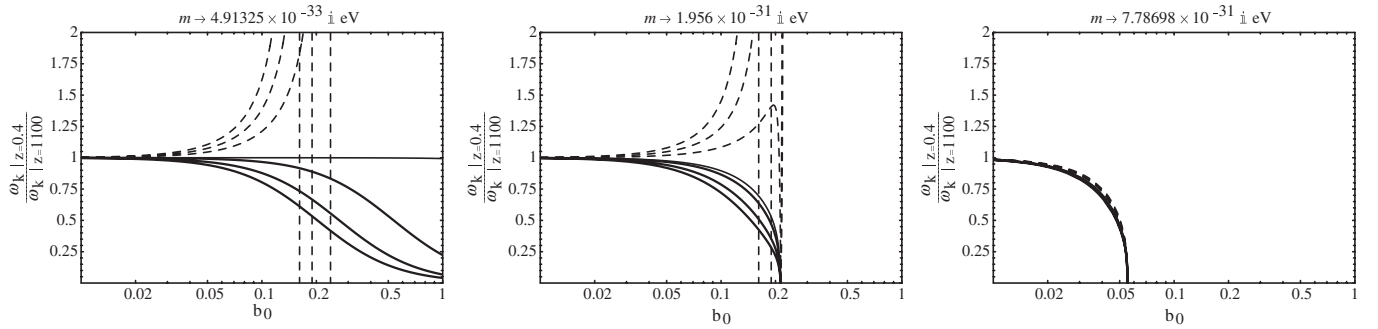


FIG. 4. Matter Domination $m^2 < 0$ WKB: Dashed curves are for $\xi < 1/6$, and thick curves are for $\xi > 1/6$.

deviation from the classical redshift formula is very small until length scales of the size $\sim 0.6cH_0^{-1}$. For imaginary mass, when $\Im(m) \lesssim 10^{-32}$ eV, the ratio of frequencies exhibits similar behavior Fig. 2. In both cases, as the magnitude of the mass of a scalar field gets larger than roughly 10^{-32} eV, it dominates the effects of ξ if $\xi \lesssim 1$. In the matter-dominated case, both real Fig. 3, and imaginary Fig. 4 masses of order $\sim |10^{31}|$ eV dominate effects when $\xi \lesssim 1$. The corrections become substantial at smaller length scales $\sim 0.1cH_0^{-1}$.

IV. WMAP FIT AND DISCUSSION

Now let us discuss the processing of the density perturbation spectrum. As is well known, once a perturbation comes within the horizon, it begins to oscillate. This phenomenon is reflected in the observed large ℓ WMAP CMB spectrum, where the first maximum (first acoustic peak) is at $\ell \sim 200$, and higher order peaks are at larger ℓ value. The low ℓ values have not been inside the horizon long enough for much processing to have taken place. The region from roughly $\ell = 20$ to $\ell = 200$ is just now beginning to undergo its first plasma oscillation, while for $\ell \lesssim 20$ very little has happened yet. But this is just the region of interest for the dispersive effects we have been discussing, and we are lucky that in this region ($\ell \lesssim 20$) we have a pristine, unprocessed spectrum. (Recall for large ℓ , we have short wavelengths, and so virtually no dispersion.)

Hence we can confine ourselves to the analysis of perturbations with wavelengths of the order of or somewhat less than the horizon size where we do not need to worry about plasma oscillations. (There may be issues of reionization to consider, but at the level we are working we choose to ignore such effects.)

Perturbations that are of the order of the horizon size today have undergone an evolution from the time of their production. A typical scenario would be: Perturbations are produced during a vacuum-dominated epoch of inflation, and are pushed outside the horizon. Inflation then ends, and the universe becomes radiation dominated. Some perturbations come back inside the horizon, are processed via plasma oscillations, etc., until about $z = 1100$, when the universe becomes matter-dominated. More perturbations re-enter the horizon and are processed until around $z = 0.4$ when the universe again becomes vacuum-dominated and perturbations again start to be pushed outside the horizon. Ultimately, we would like to follow the entire evolution of a perturbation from its production until today for modes that are currently near horizon size (an $\ell \lesssim 20$ mode). However, this would require a detailed model of the early universe. A less ambitious approach is to follow some (better understood) fraction of the evolution to demonstrate that dispersion can play a role in understanding the observational data, and leave it to future work, when a more detailed understanding of the early Universe including details of early Universe phase transitions are known, to

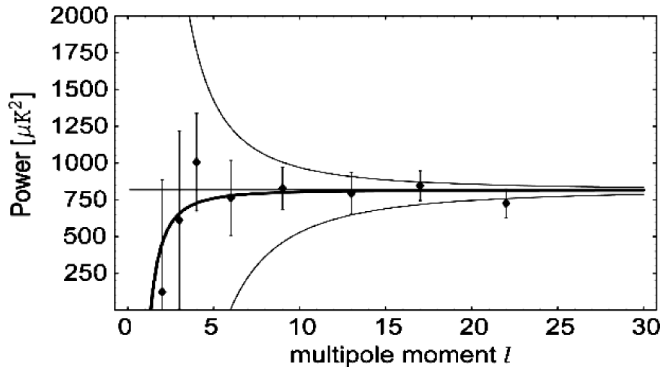


FIG. 5. Fit of the low ℓ part of WMAP spectrum to scalar fields with dispersion. The thick line is for the best fit value, $\xi = 0.166434$. We have added three other curves for comparison. The upper thin line is for $\xi = 0.169492$, the flat line is for $\xi = 1/6$, and the lower thin line is for $\xi = 0.161290$.

follow the complete evolution of the modes. To this end we have shown in Fig. 5 (where we convert wavenumber k to multipole moment ℓ using $k = \ell/(cH_0^{-1})$) the results of evolving modes from² $z = 1100$ until today (i.e. from $z = 1100$ to $z = 0.4$ with matter domination, and from $z = 0.4$ until today ($z = 0$) with vacuum domination), and have fit the results to the low ℓ WMAP data. Since an $\ell = 20$ mode undergoes very little processing or dispersive evolution, we have normalized our amplitude to this region of the spectrum. Once this is done, we have a single free parameter ξ for massless scalar fields ϕ . We then do a one-parameter fit, as shown in Fig. 5, and find $\xi \approx \frac{1}{6} - 0.0002$ see Fig. 6. This is very close to the conformal value $\xi = \frac{1}{6}$ and can be shifted there, but only at the expense of introducing a small negative mass squared for the scalar field as can be seen from the field Eq. (12) evaluated for the VDU

$$\ddot{f}_k(\eta) + \left[\beta^2 + \frac{(12\xi - 2) + (mc/a_{\text{vac}}^0)^2}{\eta^2} \right] f_k = 0. \quad (30)$$

It is clear that one can introduce the effective coupling $\bar{\xi}$ such that

$$12\bar{\xi} = 12\xi + \left(\frac{mc}{a_{\text{vac}}^0} \right)^2, \quad (31)$$

and by setting $\bar{\xi}$ to the conformal value $1/6$ we can find the value of mass m corresponding to a field ϕ with an effective conformal coupling to gravity. Our conclusion is that the evolution of large ℓ scalar modes can be used to constrain the coupling of k -essence or holographic type scalar fields to gravity, if they contribute substantially to the density perturbations [12]. For such fields, if we set $m = 0$ we find that minimally coupled field ($\xi = 0$) is

²For more precise z values see [11].

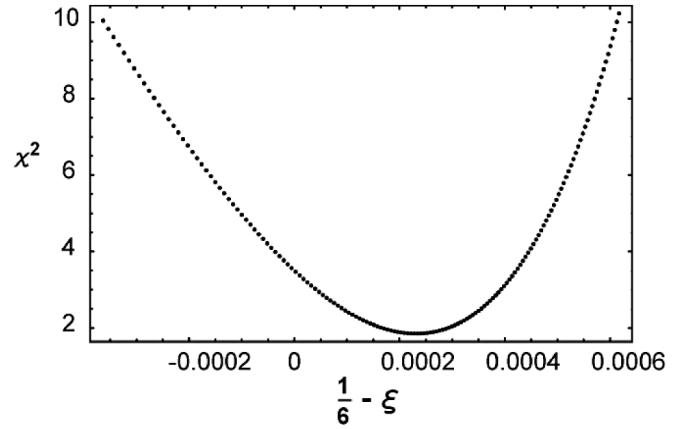


FIG. 6. Deviation of ξ from the conformal value of coupling $\xi = \frac{1}{6}$ as seen on a plot of χ^2 vs $(\frac{1}{6} - \xi)$.

easily excluded. Our fit is merely an example of how constraints on ξ can arise. Specific models will give specific results. It is interesting that, with a few assumptions, a value of ξ can in principle be extracted from a study of the cosmic microwave background. The coupling of scalar fields to gravity have other ramifications that would need to be considered in any realistic model. Another reason for being cautious about drawing sweeping inferences from Fig. 5 is that the single scalar-field action given in (2) with $m^2 = 0$ leads to a spectral index in disagreement with the data. Perhaps what one should conclude is that we need a theory with a sufficiently complicated potential $V(\phi)$ that density perturbations can be laid down when the ϕ mass is sufficiently large (see [13]), but where the late time effective theory is nearly conformally invariant, or a theory with multiple scalar moduli field.

ACKNOWLEDGMENTS

We thank Anjan Sen, Tom Weiler and Roman Buniy for helpful discussions. This work was supported in part by U.S. DOE Grant No. DE-FG05-85ER40226.

APPENDIX: VALIDITY OF WKB APPROXIMATION

The WKB approximation works best for couplings close to the conformal case $\xi = 1/6$. For various choices of parameters, we show the percent errors of the WKB approximation relative to the exact vacuum-dominated era results Fig. 7(a) and 8(a), and to the matter-dominated universe in Fig. 7(b) and 8(b).

In a matter domination universe represented in Fig. 8(b), the WKB approximation is better (i.e. up to larger scales) for positive couplings. However, the broad range of applicability of the WKB method allows us to use the WKB approximation to draw conclusions about trends in the data.

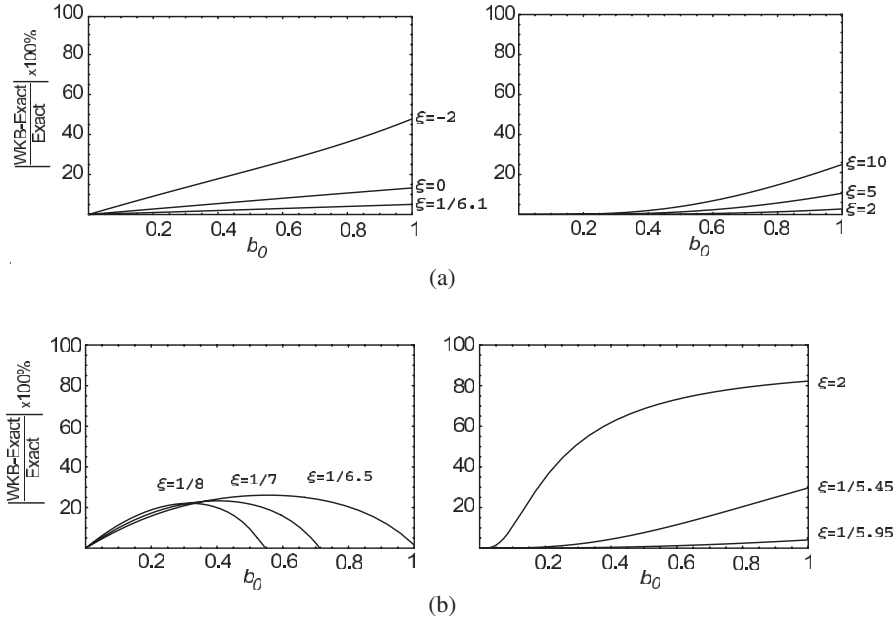


FIG. 7. Percent error in VDU (a) and MDU (b) for both negative and positive values of ξ .

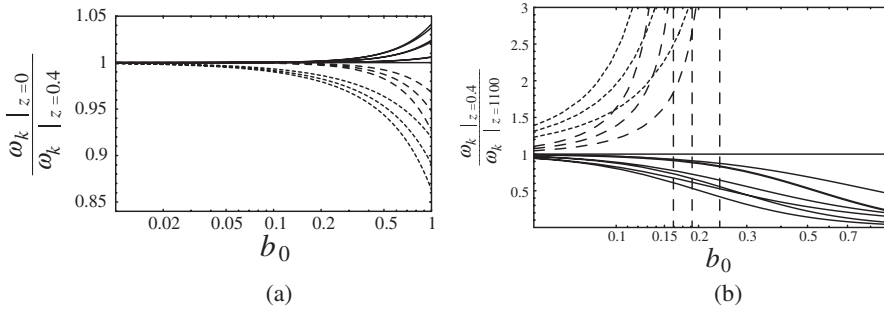


FIG. 8. Comparison of exact solutions to the WKB approximation in VDU (a) and MDU (b) case. Thin (thick) lines represent exact (WKB) solutions with $\xi > 1/6$. Small (large) dashed lines represent exact (WKB) with $\xi < 1/6$.

[1] E. W. Kolb, S. Matarrese, A. Notari, and A. Riotto, hep-th/0503117; D.H. Coule, *Classical Quantum Gravity* **22**, R125 (2005); L. Knox, *Phys. Rev. D* **73**, 023503 (2006); D. f. Zeng and Y. h. Gao, hep-th/0503154; D. L. Wiltshire, gr-qc/0503099; G. Geshnizjani, D. J. H. Chung, and N. Afshordi, *Phys. Rev. D* **72**, 023517 (2005); E. E. Flanagan, *Phys. Rev. D* **71**, 103521 (2005); C. M. Hirata and U. Seljak, *Phys. Rev. D* **72**, 083501 (2005); A. Notari, astro-ph/0503715; J. W. Moffat, astro-ph/0504004; S. Rasanen, *Classical Quantum Gravity* **23**, 1823 (2006); B. M. N. Carter, B. M. Leith, S. C. C. Ng, A. B. Nielsen, and D. L. Wiltshire, astro-ph/0504192; S. P. Patil, hep-th/0504145; E. R. Siegel and J. N. Fry, *Astrophys. J.* **628**, L1 (2005); A. A. Coley, N. Pelavas, and R. M. Zalaletdinov, *Phys. Rev. Lett.* **95**, 151102 (2005); P. Martineau and R. H. Brandenberger, *Phys. Rev. D* **72**, 023507 (2005); J. W. Moffat, astro-ph/0505326; M. Giovannini, *Phys. Lett. B* **634**, 1 (2006); D. f. Zeng and Y. h. Gao, gr-qc/0506054; V. F. Cardone, A. Troisi, and S. Capozziello, *Phys. Rev. D* **72**, 043501 (2005); H. Alnes, M. Amarzguioui, and O. Gron, astro-ph/0506449; E. W. Kolb, S. Matarrese, and A. Riotto, astro-ph/0506534; D. f. Zeng and H. j. Zhao, gr-qc/0506115; M. Giovannini, *J. Cosmol. Astropart. Phys.* **09** (2005) 009.

[2] C. L. Bennett *et al.*, *Astrophys. J. Suppl. Ser.* **148**, 1 (2003).

[3] D. Hochberg and T. W. Kephart, *Phys. Rev. Lett.* **66**, 2553 (1991).

[4] D. Hochberg and T. W. Kephart, *Phys. Rev. D* **45**, 2706 (1992).

[5] S. S. Feng, *Mod. Phys. Lett. A* **16**, 1385 (2001).

[6] V. Faraoni and E. Gunzig, *Int. J. Mod. Phys. D* **8**, 177 (1999).

[7] V. Faraoni, E. Gunzig, and P. Nardone, *Fundam. Cosm. Phys.* **20**, 121 (1999).

- [8] V. Faraoni and S. Sonego, *Phys. Lett. A* **170**, 413 (1992).
- [9] D. Hochberg and T.W. Kephart, *Phys. Rev. D* **51**, 2687 (1995).
- [10] D.N. Spergel *et al.*, astro-ph/0603449.
- [11] W. Hu and N. Sugiyama, *Astrophys. J.* **471**, 542 (1996).
- [12] M. Sasaki, *Prog. Theor. Phys.* **76**, 1036 (1986).
- [13] A.R. Liddle and D.H. Lyth, *Cosmological Inflation and Large-Scale Structure* (Cambridge University Press, Cambridge, England, 2000).